Springtail-inspired triangular laser-induced surface textures on metals using MHz ultrashort pulses

Romano, Jean-Michel; Helbig, Ralf; Fraggelakis, Fotis; Garcia Giron, Antonio; Werner, Carsten; Kling, Rainer; Dimov, Stefan

DOI:
10.1115/1.4043417

Document Version
Peer reviewed version

Citation for published version (Harvard):
Romano, J-M, Helbig, R, Fraggelakis, F, Garcia Giron, A, Werner, C, Kling, R & Dimov, S 2019, 'Springtail-inspired triangular laser-induced surface textures on metals using MHz ultrashort pulses', *Journal of Micro and Nano-Manufacturing*, vol. 7, no. 2, 024504. https://doi.org/10.1115/1.4043417

Springtail-inspired triangular laser-induced surface textures on metals using MHz ultrashort pulses

**Jean-Michel Romano (1)*, Ralf Helbig (2), Fotis Fraggelakis (3,4),
Antonio Garcia-Giron (1), Carsten Werner (2), Rainer Kling (3), Stefan Dimov (1)**

(1) Department of Mechanical Engineering, School of Engineering, University of Birmingham, B15 2TT Birmingham, United Kingdom

(2) Max Bergmann Center of Biomaterials, Leibniz Institute of Polymer Research, 01069 Dresden, Germany

(3) ALPhANOV, Technological Centre for Optics and Lasers, Optic Institute of Aquitaine, Rue F. Mitterrand, 33400 Talence, France

(4) CELIA, University of Bordeaux – CNRS – CEA UMR5107, 33405 Talence, France

* Contact: jean-michel.romano@gadz.org

Abstract

Considering the attractive surface functionalities of springtails (Collembola), an attempt at mimicking their cuticular topography on metals is proposed. An efficient single-step manufacturing process has been considered, involving Laser-Induced Periodic Surface Structures (LIPSS) generated by near-infrared femtosecond laser pulses. By investigating the influence of number of pulses and pulse fluence, extraordinarily uniform triangular structures were fabricated on stainless steel and titanium alloy surfaces, resembling the primary comb-like surface structure of springtails. The laser-textured metallic surfaces exhibited hydrophobic properties and light scattering effects that were considered in this research as a potential in-line process monitoring solution. The possibilities to increase the processing throughput by employing high repetition rates in the MHz-range are also investigated.

Keywords: Biomimicry, LIPSS, wettability, light scattering, MHz processing, uniformity.

1. Introduction

Nature offers numerous inspirations for the manufacturing of smart surfaces. Springtails are good examples, as their cuticle dispose of complex topographies with superior omniphobic and anti-adhesive surface functionalities [1,2]. Especially, cuticles with hierarchical alignment of two to three levels are observed [3]:

a) bristle-like or hairy (tertiary) structures with length of some tens of microns;
b) a micron-scaled papillose (secondary) structure, which is not present on all species;
c) a submicron-scaled alignment of small granules with interconnecting ridges (called primary structure).

Recently, laser micro manufacturing has reached a new milestone, enabling the controlled generation of highly regular Laser-Induced Periodic Surface Structures (LIPSS) on metals [4] and hexagonally-aligned submicron triangular features could be fabricated [5]. Such surface structures resembles the hexagonal comb-like pattern (see Fig. 1) observed on the submicron level of half of evaluated springtail species [3]. LIPSS exhibit promising self-cleaning and decorative properties [6] and triangular LIPSS could therefore contribute to the transfer of some springtail surface properties onto manmade surfaces.

While LIPSS have a self-organizing nature, a plethora of morphologies can be generated. In particular, the so-called low-spatial frequency LIPSS (LSFL) are a type of LIPSS that are usually quasi-periodic in the shape of wavy ripples, nanogratings or nanobubbles. Their generation can be tailored depending on irradiated materials, laser wavelength, beam polarization, fluence and number of pulses [7]. More complex LIPSS morphologies, such as diamond-shaped LSFL, were generated in multi-step processes requiring several cross-polarized scans of the surface [8]. Other single-scan processes, involving radial polarized beam, dynamic rotation of the polarization or double cross-polarized pulses, could induce complex but controlled LIPSS morphologies such as rhombic shapes [9,10].

To enable scale up manufacture of triangular LIPSS, several aspects should be addressed, such as high processing time and the development of in-line monitoring solutions. In this research, a conventional circular-polarized beam delivery set-up is used in a single raster scan mode to investigate their generation on stainless steel and titanium samples. Near-infrared femtosecond laser pulses with Gaussian-shaped intensity with high repetition rates in the MHz range are used to generate uniform springtail-inspired triangular LIPSS over large areas. Surface functionalities in term of wetting and light scattering, as well as its use as an in-line monitoring method, are discussed.

2. Experimental set-up

Stainless steel (X6Cr17) and Titanium alloy (Ti-6Al-4V) in the form of 0.7 mm- and 2 mm-thick plates and as-received roughness of 35 nm and 450 nm, respectively, are used in this research. The metallic substrates are processed using ultrashort laser pulses with 1032 nm central wavelength (λ) and 310 fs pulse duration. The beam was right-hand circularly polarized and deflected over the surface at normal incidence. The spot diameter ($2\omega_0$) is estimated experimentally to be 30 µm at $1/e^2$. The experimental set-up and raster scan strategy are depicted in Figure 2, where the pulse-to-pulse distance (d) equals the scanning speed (v) over the pulse repetition rate (f).

The following results are based on a preliminary study where a single raster scan was used to generate triangular LIPSS on steel surfaces [5]. Uniform triangles were obtained over relatively large area by varying the fluence per pulse (φ_0) and the number of pulses (N). By estimating the effective number of pulses per unit area (as in Eq. 1), an accumulated fluence

(φ) can also be calculated (see Eq. 2). The processing parameters used in the investigation are listed in Table 1.

$$N = \pi \omega_0^2 / (d\ h) \quad (1)$$

$$\varphi = N \varphi_0 = N P / (f \pi \omega_0^2) \quad (2)$$

Table 1. Laser processing parameters.

Parameters	Units	Value	
		min	max
Repetition rate (f)	MHz	0.25	2
Power (P)	W	0.01	5
Pulse Energy (E)	µJ	0.05	3.50
Fluence per pulse (φ_0)	mJ/cm^2	10	500
Scanning speed (v)	m/s	0.1	5
Hatch distance (h)	µm	1	20

Laser texturing was performed in atmospheric conditions. Any processing debris were removed by using compressed air. LIPSS morphologies were inspected using optical microscope (Alicona G5) and scanning electron microscope (ESEM Philips XL-30). The LIPSS periodicities were measured on Fast Fourier Transform (FFT), performed with the Gwyddion software. Samples were stored in polyethylene bags and wetting properties were measured with 6 µl Milli-Q water on an optical tensiometer (Attension Biolin Scientific Theta T2000-Basic+).

3. Results

3.1 Fabrication of springtail-inspired LIPSS

The surface texturing in this research was specifically designed for generating uniform submicron-scale LIPSS over large areas. Therefore, a processing window with enough pulse overlap was chosen where no rim effect due to the Gaussian energy distribution could be noticed, i.e. in the present case for h and d inferior to $\omega_0/3$. Accumulated fluence above materials' damage threshold was used to generate different LIPSS morphologies by varying the fluence per pulse and the number of pulses (see Fig. 3). All generated LIPSS in this study have multi-directional spatial periodicities that are due to the used circular polarization. These LIPSS are mainly so-called low spatial frequency LIPSS, with periodicities ranging from 0.85 to 0.98 λ.

The LIPSS seem to go through sharp morphological transitions under specific irradiation conditions, containing surprisingly uniform hexagonal alignments therebetween. While the mechanisms underlying LIPSS formations are yet to be fully understood, with such concepts put forward as surface-scattered interferences [11] or resonance of surface plasmon polaritons [12], circular polarisation is the main underlining reason for creating such hexagonal alignments [5]. A cartography of the low spatial frequency LIPSS is therefore presented in Figure 4. The mapping was done by varying the fluence per pulse and the number of pulses while keeping the other parameters constant, especially the repetition rate at 250 kHz. Uniform triangular LIPSS were produced within a processing window of 118 to 353 pulses at fluences from 71 to 144 mJ/cm^2.

The uniformity of the surface structures was observed at different micro and sub-micron scales (see Fig. 5). The hexagonally aligned LIPSSs that were generated in the selected processing

window were composed of different types of self-organised structures, as depicted in Figure 5c. For these specific processing parameters, LSFL are shaped as comb-aligned triangles with sides between 450 and 650 nm and a periodicity of 930 nm. Between the triangles, orthogonal gratings of around 80 nm periodicity could be observed. Finally, the surface was also randomly covered by nanobubbles with diameters estimated to be in the range from 40 to 150 nm. Similar triangular LIPSS were fabricated on titanium alloy substrates, which indicates that such morphologies could be achieved on other metals, too (see Fig. 6). However, the relatively rougher surface finish seems to alter the overall quality of the hexagonal arrangement.

The highest processing rate attained in the investigated processing window was 1.5 mm^2/s. Higher processing rates could be achieved by increasing both the beam deflection speed and the pulse repetition rate. To match the same range of pulse numbers while using velocities above 1m/s, repetition rates in the MHz regime had to be deployed. At 1 MHz, uniform triangular LIPSS were still observed, however with some distortions appearing. Up to 2 MHz it was possible to achieve relatively uniform triangular LIPSS on steel substrates. Thus, the processing rate could therefore be increased to 10 mm^2/s. Nevertheless, at such high repetition rates, a potential heat accumulation can occur [13] and this may explain partially some “melted-like” effects on the hexagons and the observed groove-like structures (see Fig. 7).

3.2 Surface functionalization

The uniform triangular LIPSS presented in this study could be fabricated over areas up to 40 x 40 mm^2, suggesting that the entire field of view of galvo scanners equipped with telecentric lenses could be fabricated in a single-step process. A surface of 500 mm^2 presented in Figure 8a exhibited visually uniform light scattering effect. White light was producing rainbow colours depending on the illumination and observation angles. Rhombic-shaped LIPSS were shown to produce such diffracting colours in 2 symmetric directions [9]. In the case of submicron hexagonal arrangements, under normal illumination, light was diffracted in 6 main directions, as the Fourier Transforms (see Fig. 3c and 6a) were suggesting. Furthermore, logos of smaller dimensions could be produced with a similar structural colorization (see Fig. 8b).

The wettability of the textured metallic substrates was analysed in term of the static water contact angle. The textured samples became hydrophilic right after laser processing and the static contact angle (θ) followed a progressive grow (see Eq. 3) and then stabilising at a maximum value (θ_{eq}) [14]:

$$\theta(t) = \theta_{eq} \cdot (1-e^{-t}/\beta) \quad (3)$$

where β is a time constant. Both steel and titanium alloy samples exhibited similar ageing behaviours. For stainless steel, the maximum contact angle was measured at more than 155° after 7 days of storage in ambient air [5] or after the same amount of time in plastic bags (see Fig. 8c-d). It should be noted that after ageing all LIPSS structures in this study exhibited the same isotropic superhydrophobic state with static contact angles higher than 150° and low rolling off angles (<10°).

The triangular LIPSS fabricated using MHz repetition rates, as described in Section 3.1, had similar wetting properties as those produced employing kHz processing, even on samples with non-hexagonal aligned textures. Only the optical properties were affected either because the beam dynamics were not correctly adjusted for the higher scanning speeds, or the triangular LIPSS became locally misaligned (see Fig. 9).

3.3 Comparison to the springtail cuticle

The springtails presented in the introduction exhibit a hierarchical surface structure whereas the smallest structure level represents the most interesting morphological features for anti-wetting and anti-bioadhesion applications. Figure 1c illustrates these submicron-scaled structure with, in average, equilateral triangles of 265 nm sides and 500 nm spatial periodicity. Using 1032 nm ultra short laser pulses, the comb-aligned triangles were two times larger than the springtail (see Section 3.1). Reducing the laser wavelength [4] or preliminary surface texturing [15] may generate smaller spatial LSFL periodicities that are closer to the springtail dimensions. Smaller dimensions are foreseen to lead to lower initial bioadhesion [16], for instance.

Nevertheless, up-scaling the springtail comb-pattern to periodicities in the range from 850 nm to 1 µm can enable light-scattering effects that are not present on the springtail cuticles. Therefore, tailored triangular LIPSS could find potential applications in decoration and/or anti-counterfeiting, too. In addition, potential in-line optical or scattering monitoring techniques were used for linear LSFL [17,18] and could be developed to ensure that the triangular LIPSS process is kept in control during MHz processing. Indeed, the 3 symmetrical scattering directions, as shown on the FFTs on Fig. 3c and 6a, could be easily monitored e.g. by the correct angular positioning of a collimated light source and a range of photodiode. Deviation from the 3-directional scattering profile, as seen on the FFT, would mean triangles are not anymore produced.

Finally, it is worth mentioning that the textured surfaces were not omni- or lyophobic, as it is usually the case for springtails, due to the presence of overhanging granules [1]. LIPSS, especially LSFL, are not yet known to generate such undercuts.

4. Conclusions

Triangular LIPSS were fabricated on metallic surfaces using circularly polarized near-infrared femtosecond laser pulses in a one-step process. The large area surface texturing with such LIPSS was investigated on stainless steel and titanium substrates by varying the number of pulses and fluence in a narrow, however repeatable, processing window. It was shown that processing rates up to 10 mm^2/s were achievable by employing a MHz laser processing. At the same time the limitations of such high dynamics processing were highlighted. The resulting triangular LIPSS resemble, to some extent, the cuticle topography of some springtails' species that incorporate twice smaller triangular hexagonally-aligned structures. Superhydrophobicity were demonstrated on laser textured metals that could be deployed for engineering easy-to-clean surfaces. Light scattering could be useful to display structural colours and for inline monitoring of LIPSS processing.

Acknowledgments

The work was carried out within the H2020 "European ESRs Network on Short Pulsed Laser Micro/Nanostructuring of Surfaces for Improved Functional Applications" (Laser4Fun) under the ITN Marie Skłodowska-Curie grant agreement No. 675063 (www.laser4fun.eu), the H2020 FoF programme "High-Impact Injection Moulding Platform for mass-production of 3D and/or large micro-structured surfaces with Antimicrobial, Self-cleaning, Anti-scratch, Anti-squeak and Aesthetic functionalities" (HIMALAIA), and of the UKIERI DST programme "Surface functionalisation for food, packaging, and healthcare applications".

Figures

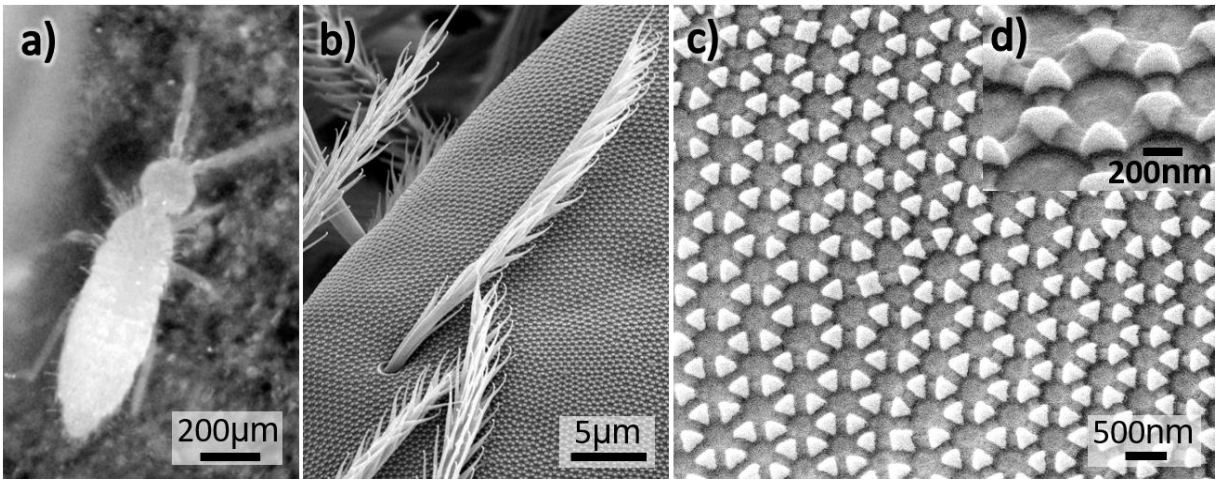

Figure 1. Springtail: specimen of *Sinella tenebricosa* (a) with micro- (b) and submicro- scale (c) close up. Tilted view of a hexagonal arrangement of granules and ridges (d).

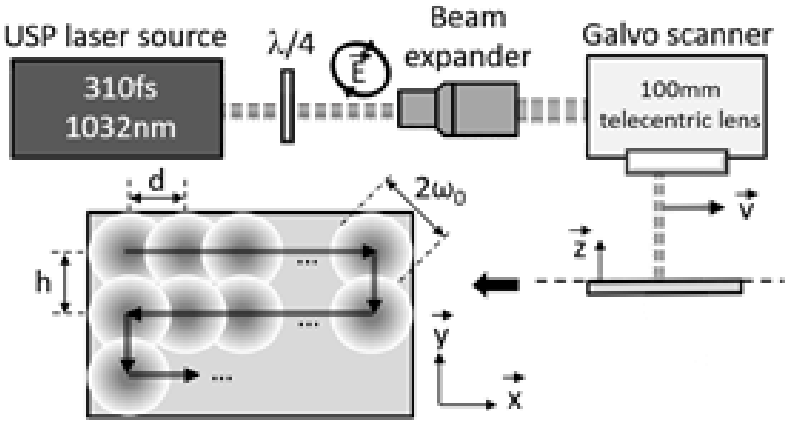

Figure 2. Beam line components and raster scan strategy.

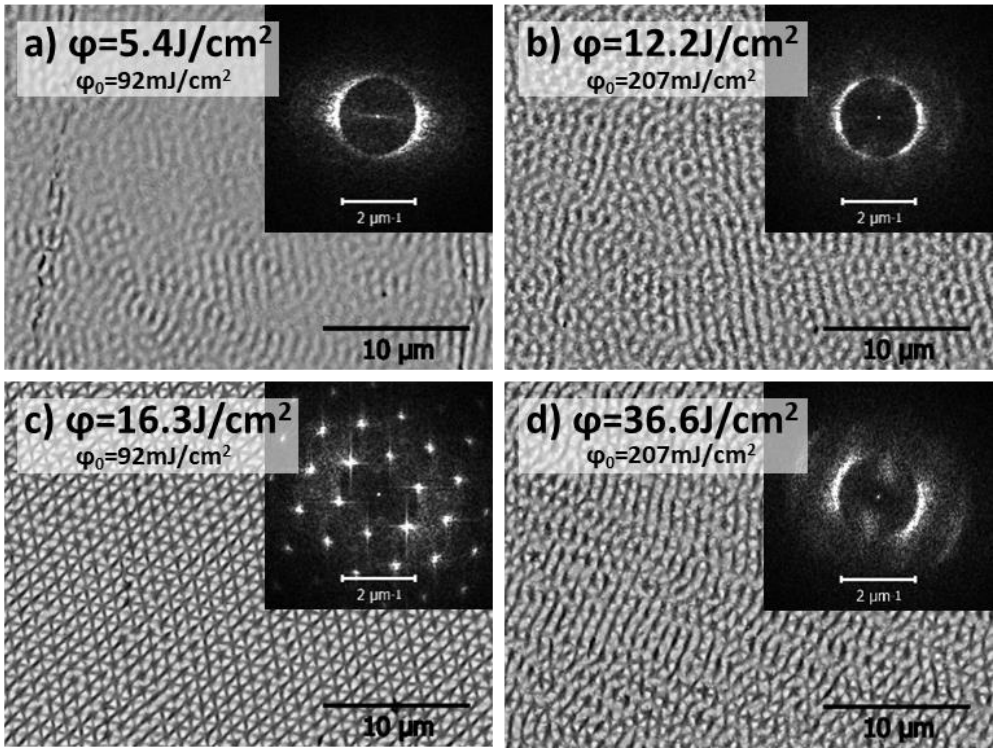

Figure 3. SEM pictures and corresponding FFTs illustrating the LIPSS evolution with fluence increase (h=2µm) on X6Cr17, for N=59 (a-b) and N=177 (c-d).

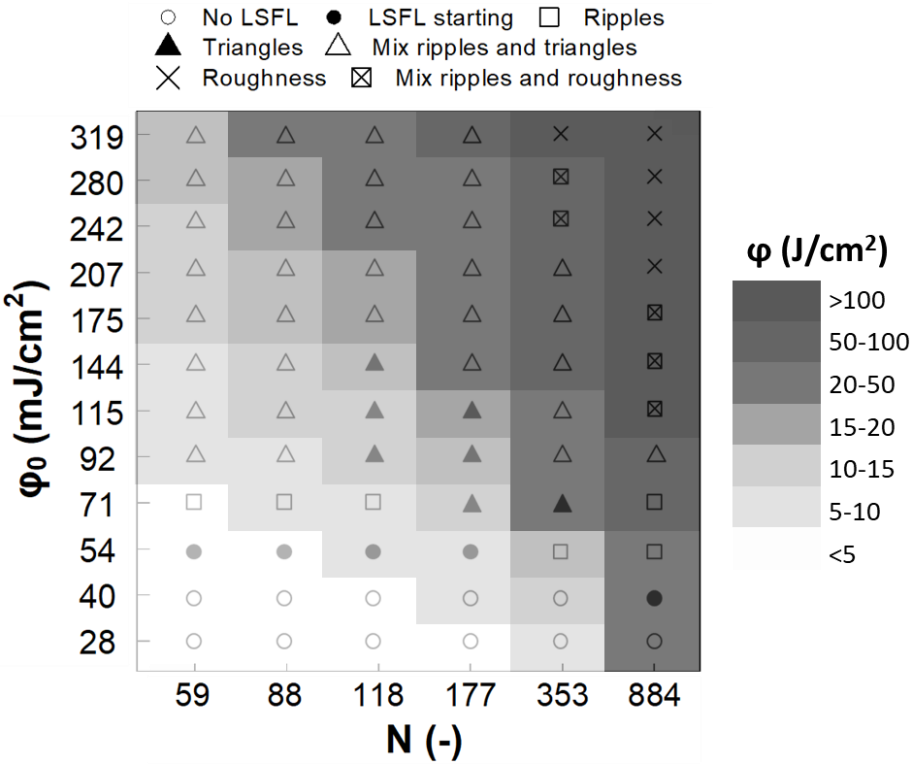

Figure 4. Evolution of LIPSS morphologies on X6Cr17 with number of pulses and fluence per pulse.

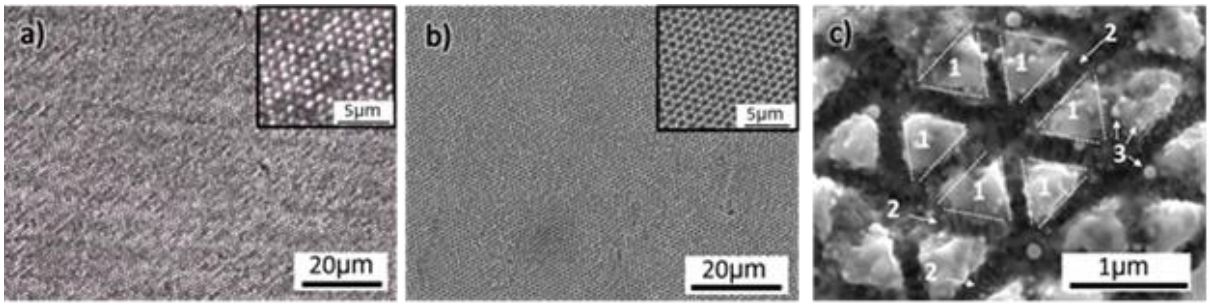

Figure 5. Optical microscope views (a) and SEM pictures (b-c) of a large-area hexagonal arrangement of triangular-LIPSS (zone 1) on X6Cr17. High spatial frequency LIPSS (zone 2) and nanobubbles (zone 3) are also highlighted.

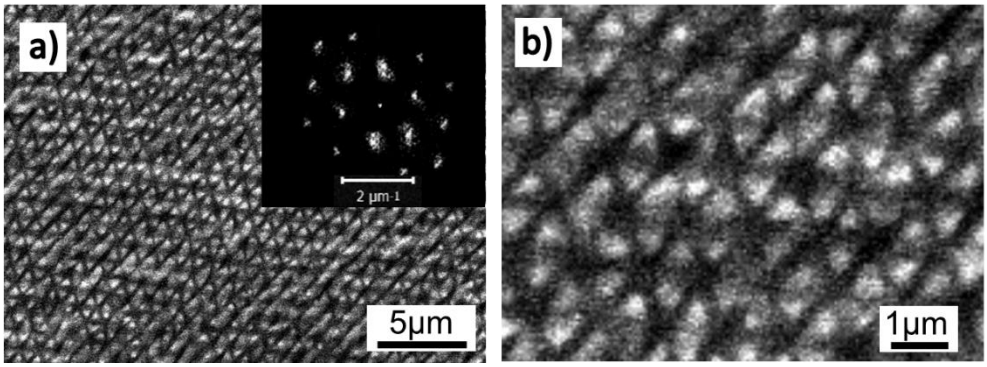

Figure 6. SEM pictures with corresponding FFT (a) and detailed view (b) of triangular LIPSS on Ti-6Al-4V (h = 2 µm, φ_0 = 54 mJ/cm^2, N = 442, φ = 23.9 J/cm^2).

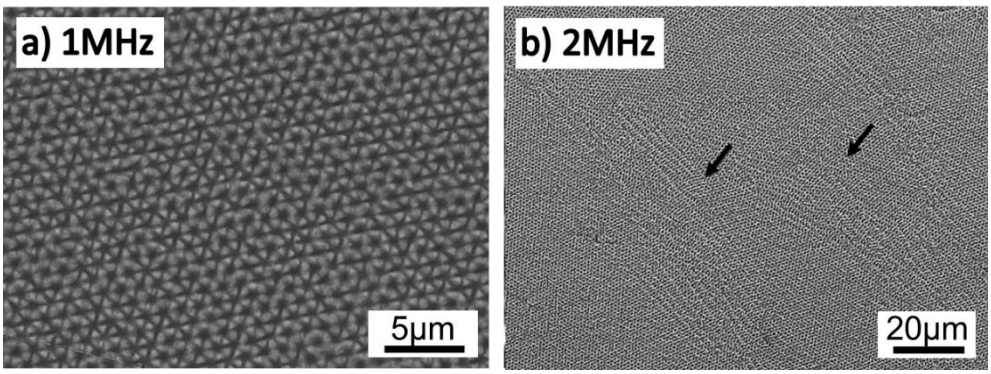

Figure 7. MHz processing of triangular LSFL on X6Cr17 at fixed h = 2 µm, φ_0 = 100 mJ/cm^2, for 118 pulses at 1 MHz (a) and 141 pulses at 2 MHz (b).

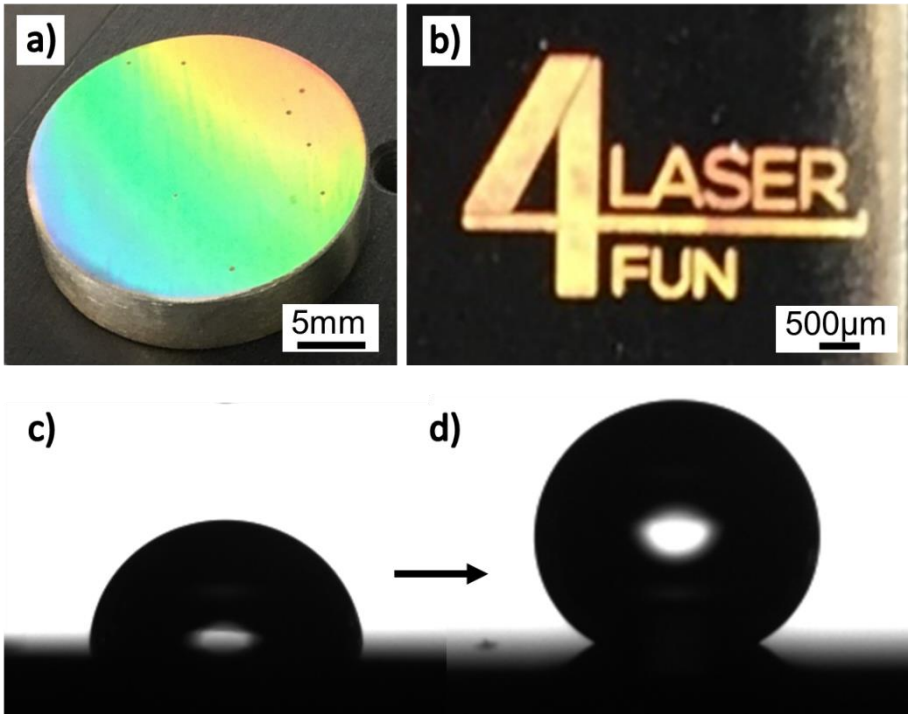

Figure 8. The uniform structural colours of triangular LIPSS over large area (a) and micro-scale logo writing (b). The contact angle of 6 µl water drops on untextured (c) compared to textured (d) X6Cr17.

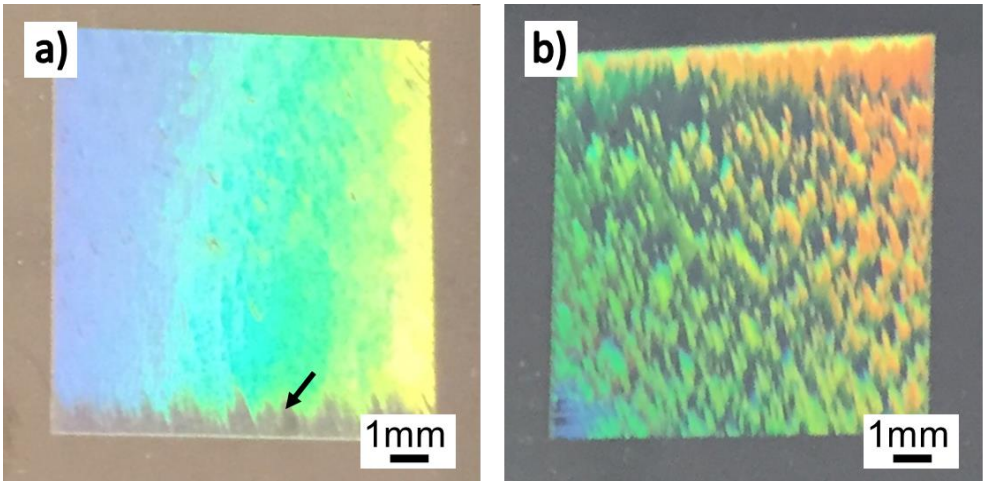

Figure 9. The visual inspection of the structural colours fabricated, at fixed φ_0 = 100 mJ/cm^2, on X6Cr17 by 118 pulses at 1 MHz, φ = 11.8 J/cm^2 (a) and 141 pulses at 2 MHz, φ = 14.1 J/cm^2 (b).

References

[1] R. Hensel, C. Neinhuis, C. Werner, The springtail cuticle as a blueprint for omniphobic surfaces, Chem. Soc. Rev. 45 (2016) 323–341. doi:10.1039/C5CS00438A.

[2] R. Helbig, J. Nickerl, C. Neinhuis, C. Werner, Smart Skin Patterns Protect Springtails, PLOS ONE. 6 (2011) e25105. doi:10.1371/journal.pone.0025105.

[3] J. Nickerl, R. Helbig, H.-J. Schulz, C. Werner, C. Neinhuis, Diversity and potential correlations to the function of Collembola cuticle structures, Zoomorphology. 132 (2013) 183–195. doi:10.1007/s00435-012-0181-0.

[4] I. Gnilitskyi, L. Orazi, N.M. Bulgakova, T.J.-Y. Derrien, T. Mocek, Y. Levy, High-speed manufacturing of highly regular femtosecond laser-induced periodic surface structures: physical origin of regularity, Sci. Rep. 7 (2017) 8485. doi:10.1038/s41598-017-08788-z.

[5] J.-M. Romano, A. Garcia-Giron, P. Penchev, S. Dimov, Triangular laser-induced submicron textures for functionalising stainless steel surfaces, Appl. Surf. Sci. 440 (2018) 162–169. doi:10.1016/j.apsusc.2018.01.086.

[6] A.Y. Vorobyev, C. Guo, Multifunctional surfaces produced by femtosecond laser pulses, J. Appl. Phys. 117 (2015) 033103. doi:10.1063/1.4905616.

[7] S. Graf, F.A. Muller, Polarisation-dependent generation of fs-laser induced periodic surface structures, Appl. Surf. Sci. 331 (2015) 150–155. doi:10.1016/j.apsusc.2015.01.056.

[8] A. Cunha, A.-M. Elie, L. Plawinski, A.P. Serro, A.M. Botelho do Rego, A. Almeida, M.C. Urdaci, M.-C. Durrieu, R. Vilar, Femtosecond laser surface texturing of titanium as a method to reduce the adhesion of Staphylococcus aureus and biofilm formation, Appl. Surf. Sci. 360, Part B (2016) 485–493. doi:10.1016/j.apsusc.2015.10.102.

[9] E. Skoulas, A. Manousaki, C. Fotakis, E. Stratakis, Biomimetic surface structuring using cylindrical vector femtosecond laser beams, Sci. Rep. 7 (2017) srep45114. doi:10.1038/srep45114.

[10] F. Fraggelakis, G. Mincuzzi, J. Lopez, I. Manek-Hönninger, R. Kling, 2D laser induced periodic surface structures with double cross-polarized pulses, in: Laser-Based Micro- Nanoprocessing XII, International Society for Optics and Photonics, 2018: p. 105200L. doi:10.1117/12.2287841.

[11] J.F. Young, J.S. Preston, H.M. van Driel, J.E. Sipe, Laser-induced periodic surface structure. II. Experiments on Ge, Si, Al, and brass, Phys. Rev. B. 27 (1983) 1155–1172. doi:10.1103/PhysRevB.27.1155.

[12] J. Bonse, A. Rosenfeld, J. Krüger, On the role of surface plasmon polaritons in the formation of laser-induced periodic surface structures upon irradiation of silicon by femtosecond-laser pulses, J. Appl. Phys. 106 (2009) 104910. doi:10.1063/1.3261734.

[13] F. Fraggelakis, G. Mincuzzi, J. Lopez, I. Manek-Hönninger, R. Kling, Texturing metal surface with MHz ultra-short laser pulses, Opt. Express. 25 (2017) 18131. doi:10.1364/OE.25.018131.

[14] A.-M. Kietzig, S.G. Hatzikiriakos, P. Englezos, Patterned Superhydrophobic Metallic Surfaces, Langmuir. 25 (2009) 4821–4827. doi:10.1021/la8037582.

[15] J.-M. Romano, R. Ahmed, A. Garcia-Giron, P. Penchev, H. Butt, O. Delléa, M. Sikosana, R. Helbig, C. Werner, S. Dimov, Subwavelength Direct Laser Nanopatterning via Microparticle Arrays for Functionalizing Metallic Surfaces, J. Micro Nano-Manuf. (2019). doi:10.1115/1.4042964.

[16] R. Helbig, D. Günther, J. Friedrichs, F. Rößler, A. Lasagni, C. Werner, The impact of structure dimensions on initial bacterial adhesion, Biomater Sci. 4 (2016) 1074–1078. doi:10.1039/C6BM00078A.

[17] J.G.A.B. Simões, R. Riva, W. Miyakawa, High-speed Laser-Induced Periodic Surface Structures (LIPSS) generation on stainless steel surface using a nanosecond pulsed laser, Surf. Coat. Technol. 344 (2018) 423–432. doi:10.1016/j.surfcoat.2018.03.052.

[18] J. Tian, M. Lancry, S.H. Yoo, E. Garcia-Caurel, R. Ossikovski, B. Poumellec, Study of femtosecond laser-induced circular optical properties in silica by Mueller matrix spectropolarimetry, Opt. Lett. 42 (2017) 4103. doi:10.1364/OL.42.004103.